

# Combined Effect of Poly(hydroxybutyrate) and Plasticizers on Polylactic acid Properties for Film Intended for Food Packaging

Marina P. Arrieta · María D. Samper ·  
Juan López · Alfonso Jiménez

Published online: 25 June 2014  
© Springer Science+Business Media New York 2014

**Abstract** Poly(lactic acid) PLA, and poly(hydroxybutyrate) PHB, blends were processed as films and characterized for their use in food packaging. PLA was blended with PHB to enhance the crystallinity. Therefore, PHB addition strongly increased oxygen barrier while decreased the wettability. Two different environmentally-friendly plasticizers, poly(ethylene glycol) (PEG) and acetyl(tributyl citrate) (ATBC), were added to these blends to increase their processing performance, while improving their ductile properties. ATBC showed higher plasticizer efficiency than PEG directly related to the similarity solubility parameters between ATBC and both biopolymers. Moreover, ATBC was more efficiently retained to the polymer matrix during processing than PEG. PLA–PHB–ATBC blends were homogeneous and transparent blends that showed promising performance for the preparation of films by a ready industrial process technology for food packaging applications, showing slightly amber color, improved elongation at break, enhanced oxygen barrier and decreased wettability.

**Keywords** Poly(lactic acid) · Poly(hydroxybutyrate) · Blend · Barrier properties · Ductility

---

M. P. Arrieta (✉) · M. D. Samper · J. López  
Instituto de Tecnología de Materiales, Universitat Politècnica de València, Plaza Ferrandiz y Carbonell No1, 03801 Alcoy, Alicante, Spain  
e-mail: marrieta@itm.upv.es

M. P. Arrieta  
Catholic University of Cordoba, Camino a Alta Gracia Km 7½,  
5017 Córdoba, Argentina

A. Jiménez  
Analytical Chemistry, Nutrition and Food Sciences Department,  
University of Alicante, P.O. Box 99, 03080 Alicante, Spain

## Introduction

The concerns on the environmental impact of food packaging materials after use are currently increasing by their high consumption and short shelf-life [1]. Some fractions of the plastic waste generated from food packaging materials may be recycled, but most of these residues are disposed in landfills by technical and/or economical reasons [2]. Therefore, the use of non-renewable and non-biodegradable plastics for short shelf-life applications should be considered as potentially hazardous to the environment [3, 4]. Consequently, the development of new bio-based and biodegradable packaging materials is currently growing. In this sense, poly(lactic acid) (PLA) and poly(hydroxybutyrate) (PHB) are thermoplastic bio-based polyesters with highly promising perspectives for short-life applications [5–8]. PLA is currently the most used biobased materials by the food packaging industry in disposable cutlery, plates, lids [9], cups [5], postharvest packaging of fresh vegetables [10] and fast-food containers [11]. It is obtained by fermentation of renewable agricultural sources, such as corn [12, 13], cellulose [14] and other polysaccharides [12, 15]. However, the use of PLA in flexible films is restricted by its poor ductility, thermal and barrier properties [13].

Considerable academic and industrial efforts have been focused on PLA modification for extending PLA applications in food packaging industry, such as the addition of modifiers, nanotechnology, copolymerization or blending. It is known that the increase of crystallinity level could improve the use of PLA as food packaging material, due to its direct impact on gas permeation [8]. Melt blending PLA with other polymers can lead to significant improvement of the final properties through a cost-effective, easy and readily available processing technology. PHB is a highly crystalline bio-polyester produced by controlled bacterial

fermentation [7] with relatively high melting point (173–180 °C) [3, 7] similar to that of PLA allowing physically blending both polymers in the melt state. After processing it yields stiff and brittle materials with poor mechanical properties [1, 16] and thermal degradation close to its melting point, limiting its processability [17]. These limitations have hampered the use of both biopolymers in the preparation of flexible films for food packaging.

It has been reported that the addition of PHB to PLA matrices could enhance its crystallinity [18], while PHB mechanical properties could be improved [19]. PLA–PHB blends have been widely studied during the last years [7, 8, 18–20]. For instance, Ni et al. [18] blended oligomers of 3-hydroxybutyrate (OHB) and PLA to enhance the PLA crystallization when OHB was introduced in amounts lower than 40 wt%, with phase separation at higher loadings [18]. Besides, Zhang and Thomas studied PLA–PHB blends at different mass ratios (100:0, 75:25, 50:50, 25:75, 0:100) and reported that PLA–PHB (75:25) blends showed higher mechanical properties than neat PLA [7].

The inherent brittleness of PLA and PHB makes necessary the addition of plasticizers to improve their ductile properties and to get the flexibility required for films manufacturing. It is known that compatibility between plasticizers and polymers is a major issue for effective plasticization [21]. In a previous work it was observed that the addition of *D*-limonene improved the interaction between PLA and PHB due to a plasticization effect [8]. In this sense, some works were reported where PHB was blended with poly(ethylene glycol) (PEG) [22] and citrate esters, such as acetyl tributyl citrate (ATBC) [1, 3] and both are considered as efficient plasticizers for PLA [3, 23, 24]. Moreover, the European Food Safety Authority (EFSA) reported that the use of PEG [25] and ATBC [26] do not raise a safety concern for food contact materials. It was reported that ATBC was more effective in enhancing the PLA flexibility at concentrations higher than 10 wt% [27, 28]. However, Coltelli et al. [29] reported enhanced crystallinity in PLA plasticized with ATBC at concentrations lower than 20 wt% [29]. Courgneau et al. [23] studied PLA plasticized with PEG and ATBC. They reported that the addition of ATBC at concentrations higher than 13 wt% resulted in a significant decrease in  $T_g$  and the corresponding increase in elongation at break with no phase separation up to 17 wt%, while PEG-300 showed phase separation at contents higher than 9 wt% [23]. Kulinski and Piorkowska [30] observed phase separation in PLA–PEG blends at 20 wt% of PEG-200 and 30 wt% of PEG-400 [30]. Martin and Avérous [31] reported that PEGs with low molar masses showed good miscibility with PLA matrices [31].

The aim of this work was to prepare PLA–PHB blends (75:25) for food packaging applications. These developments were focused on the reinforcement of PLA by blending with PHB to increase crystallinity and to improve barrier properties, while the addition of plasticizer aimed to increase the blend's ductility. Two different plasticizers, PEG and ATBC, were tested to produce flexible films. Structural, thermal, mechanical and oxygen barrier properties of these films were evaluated to assess the most adequate formulation for the intended application.

## Experimental

### Materials

Poly(lactic acid) (PLA) pellets (Ingeo™ 4032D,  $M_n = 217,000$  Da, 2 wt% *D*-isomer,  $M_w/M_n = 2$ ) was supplied by NatureWorks LLC (Minnetonka, MIN, USA), PHB (PHB P226,  $M_w = 426,000$  Da) was provided by Biomer (Krailling, Germany). ATBC ( $M = 402$  g mol<sup>-1</sup>, 98 % purity) and PEG ( $M_n = 300$  g mol<sup>-1</sup>) were purchased from Sigma-Aldrich (Móstoles, Madrid, Spain).

### Films Preparation and Processing

Poly(lactic acid) (PLA) pellets and plasticizers were dried overnight at 80 °C in a vacuum oven to prevent PLA hydrolysis during processing [32]. Meanwhile, PHB pellets were dried at 40 °C for 4 h. Blends were prepared by mixing PLA and PHB pellets (75:25 wt% ratio) in a Haake PolyLab QC mixer (Thermo Fischer Scientific Inc., Waltham, MA, USA), equipped with a pair of high-shear rolls, at 180 °C and rotation speed 50 rpm for 4 min. ATBC and PEG were added at 15 wt% after 3 min when PLA or PLA–PHB blends had achieved the melt state. Each blend was then processed into films by compression molding at 180 °C in a hot press (Mini C 3850, Caver, Inc., Wabash, IN, USA) by using a film mold (15 × 15 cm<sup>2</sup>). Eight gram of each blend were kept between the plates at atmospheric pressure for 2 min until melting and they were further submitted to the following pressure cycle, 3 MPa for 1 min, 5 MPa for 1 min and finally 10 MPa for 2 min with the aim to eliminate the trapped air bubbles [33]. Films were then quenched to room temperature at atmospheric pressure. Their average thickness was measured with a Digimatic Micrometer Series 293 MDC-Lite (Mitutoyo, Japan) ± 0.001 mm at ten random positions over the film surface for barrier properties testing and at five positions along the strips surface for the mechanical properties determination. The films average thickness was 200 ± 50 μm.

## Characterization

### Thermal Characterization

Thermogravimetric analysis (TGA) tests were carried out by using a TGA/SDTA 851e Mettler Toledo thermal analyzer (Schwarzenbach, Switzerland). Raw materials were heated (isothermal mode) at 180 °C for 25 min under air (flow rate 50 mL min<sup>-1</sup>) to evaluate the thermal stability of raw materials at the processing conditions. Films were heated at 10 °C min<sup>-1</sup> from 30 to 600 °C under nitrogen atmosphere (flow rate 50 mL min<sup>-1</sup>). In both cases samples masses were between 5–7 g.

Differential scanning calorimetry (DSC) tests were carried out in a DSC Q-2000 (TA Instruments, New Castle, DE, USA) under nitrogen (flow rate 50 mL min<sup>-1</sup>). Samples (around 4 mg) were introduced in aluminum pans, which were sealed with a Tzero press (TA Instruments). All tests consisted of a first heating stage from -90 to 180 °C at 10 °C min<sup>-1</sup>, followed by a cooling process up to -90 °C at the maximum rate given by the instrument and subsequent heating up to 200 °C at 10 °C min<sup>-1</sup>. Glass transition ( $T_g$ ), cold-crystallization ( $T_{cc}$ ) and melting temperatures ( $T_m$ ) were determined during the second heating scan. The degree of crystallinity ( $\chi_c$ ) was calculated by using Eq. 1, where  $\Delta H_m$  is the melting enthalpy,  $\Delta H_{cc}$  is the cold crystallization enthalpy,  $\Delta H_m^c$  is the melting heat associated to pure crystalline PLA, reported to be 93 J g<sup>-1</sup> [34] and  $W_{PLA}$  the proportion of PLA in the blend.

$$\chi_c = 100\% \times \left[ \frac{\Delta H_m - \Delta H_c}{\Delta H_m^c} \right] \times \frac{1}{W_{PLA}} \quad (1)$$

For the neat PHB film the  $\chi_c$  was calculated by following the Eq. 2, where  $\Delta H_m^c$  is the melting heat associated to pure crystalline PHB, reported to be 146 J g<sup>-1</sup> [35].

$$\chi_c = 100\% \times \left[ \frac{\Delta H_m}{\Delta H_m^c} \right] \quad (2)$$

### Scanning Electron Microscopy (SEM)

Scanning Electron Microscopy (SEM) micrographs of both, surface and cross-section areas after tensile tests, were obtained with a Phenom SEM (FEI Company, Eindhoven, The Netherlands), operated at 10 kV. Samples were coated with a gold layer (10–25 nm thickness) in vacuum conditions prior to their analysis to increase their electrical conductivity. Micrographs were registered at 1,000 × magnification.

### Mechanical Characterization

Tensile tests were carried out at room temperature with a IBERTEST ELIB 30 (S.A.E. Ibertest, Madrid, Spain) machine by following the ASTM D882-01 Standard [36]. Tests were performed in rectangular strips (dimensions:

100 × 10 mm<sup>2</sup>), initial grip separation 50 mm, crosshead speed 25 mm min<sup>-1</sup> and load cell 5 kN. The average percentage deformation at break ( $\epsilon_B$  %), elastic modulus ( $E$ ) and tensile strength (TS) were calculated from the resulting stress–strain curves as the average of five measurements from three films of each composition.

### Oxygen Transmission Rate (OTR)

Oxygen Transmission Rate (OTR) measurements were carried out with an 8,500 oxygen permeation analyzer (Systech Instruments, Metrotec, SA, Spain). Circular films (140 mm diameter) were conditioned at 50 ± 2 % relative humidity and 25.0 ± 0.1 °C prior to testing. Pure oxygen (99.9 %) was introduced into the upper half of the chamber while pure nitrogen was injected into the lower half where one oxygen sensor is placed. Values were expressed as OTR· $e$  where  $e$  is the film thickness (mm).

### Total Soluble Matter (TSM)

Total soluble matter (TSM) was determined as the percentage in dry basis of every sample solubilized in distilled water after 24 h [37] and it was calculated by using Eq. 3:

$$TSM = 100 \times \frac{m_0 - m_f}{m_0} \quad (3)$$

where  $m_0$  is the initial dry weight of a square sample (20 × 20 mm<sup>2</sup>) calculated after drying in an air-circulating oven at 105 °C for 24 h. Samples were then immersed in 30 mL of a 0.02 % (w/w) aqueous sodium azide solution at room temperature for 24 h. Samples were further rinsed with distilled water, dried at 105 °C and re-weighed until constant weight (±0.0001 g) to determine the final weight ( $m_f$ ). Three films of each composition were tested and the average value was determined as the TSM. Sample weights were determined with an AG-245 Mettler Toledo analytical balance.

### Water Contact Angle

A standard goniometer (EasyDrop-FM140, KRÜSS GmbH, Hamburg, Germany) equipped with a camera and Drop Shape Analysis SW21; DSA1 software was used to test the water contact angle ( $\theta^\circ$ ) at room temperature. The contact angle was determined by randomly putting 6 drops of distiller water ( $\approx 2$  μL) onto the films surface with a syringe and the average values of ten measurements for each drop were calculated [4].

### Film Transparency and Color

These properties were evaluated by using a COLORFLEX-DIFF2 45°/0° HunterLab colorimeter, (Hunter Associates

Laboratory Inc., Reston, VI, USA). The instrument was calibrated with a white standard tile and the average value of five measurements at random positions over the samples surface (20 × 20 mm<sup>2</sup>) was calculated. Transparency was calculated by following Eq. 4:

$$Transparency = \frac{A_{600}}{e} \tag{4}$$

where A<sub>600</sub> is the absorbance at 600 nm and e the film thickness (mm) [38].

The color coordinates, L (lightness), a\* (red–green) and b\* (yellow–blue) were used to determine the total color differences (ΔE) induced by the presence of plasticizer in films when compared to the control PLA or PLA–PHB formulations by following Eq. 5:

$$\Delta E_{CIE}^* = \sqrt{(\Delta L)^2 + (\Delta a^*)^2 + (\Delta b^*)^2} \tag{5}$$

Yellowness index (YI) was used to evaluate the color change from clear to yellow.

### Statistical analysis

Significance in the data differences were statistically analyzed by one-way variance analysis (ANOVA) by using Origin-Pro 8 software. Tukey’s test with a 95 % confidence level was used to identify which data groups were significantly different from others.

## Results and Discussion

### Blends Preparation and Homogeneity

It is known that the effective blending of two polymers requires high affinity between them. Two substances with similar solubility parameters (δ) should be mutually soluble [39]. This effect can be predicted by calculating their respective δ values [5], calculated by following Eq. 6.

$$\delta = \frac{D \sum G}{M} \tag{6}$$

where δ ((cal cm<sup>-3</sup>)<sup>1/2</sup>) is the solubility parameter for each component, D (g cm<sup>-3</sup>) is the density, G ((cal cm<sup>-3</sup>)<sup>1/2</sup>mol<sup>-1</sup>) is the group molar cohesive energy and M (g mol<sup>-1</sup>) is the molar mass per repetitive unit. The PLA solubility parameter has been reported to range between 19.5 and 20.5 MPa<sup>1/2</sup> [5], while the solubility parameter for PHB ranges between 18.5 and 20.1 MPa<sup>1/2</sup> [16]. Differences are relatively low and consequently good miscibility between both polymers should be expected.

In the case of plasticizers, they should be compatible with the polymer matrix [40, 41], and the relative affinity of the polymer and plasticizer can be assessed by

**Table 1** Film formulations prepared in this study

Film designation	PLA (wt%)	PHB (wt%)	PEG (wt%)	ATBC (wt%)
PLA	100	–	–	–
PLA–PEG	85	–	15	–
PLA–ATBC	85	–	–	15
PHB	100	–	–	–
PLA–PHB	75	25	–	–
PLA–PHB–PEG	63.75	21.25	15	–
PLA–PHB–ATBC	63.75	21.25	–	15

calculating their δ values [39]. The solubility parameters for PEG and ATBC were calculated as 16.7 and 20.2 MPa<sup>1/2</sup>, respectively. Therefore, since ATBC shows solubility parameter close to PLA and PHB values, good miscibility should be expected. The addition of PEG to the PLA–PHB matrix was also checked, since their δ values are in the same order of magnitude. Seven different plasticized and unplasticized PLA and PLA–PHB films were prepared as summarized in Table 1 and their aspect is shown in Fig. 1. All films were mostly transparent and colorless except those with high amounts of PHB in their formulations. These differences in color will be further discussed.

### Thermal Characterization

#### Thermogravimetric Analysis (TGA)

The thermal stability of raw materials at the blends processing temperature (180 °C) is shown in Fig. 2a. As expected, while both polymers did not show significant weight losses at this temperature, some plasticizer evaporation was observed, suggesting possibilities of plasticizer losses during processing. ATBC showed higher thermal stability at the processing temperature than PEG. However, the actual weight loss was low in both cases, since their losses were lower than 0.5 % after one minute at 180 °C. Figure. 2b shows the TGA curves of all blends at 180 °C. It was observed that both plasticizers improved the thermal stability of the PLA–PHB blend for times lower than 9 min. All samples showed a weight loss lower than 1 % after 6 min, which is the actual time that blends were processed into films. Plasticized PLA and plasticized PLA–PHB formulations with ATBC were slightly more thermally stable than those with PEG.

Thermogravimetric analysis (TGA) curves representing the thermal behavior of plasticized PLA and PLA–PHB blends are plotted in Fig. 2c, d, respectively. The main thermal parameters obtained from these curves are summarized in Table 2. As expected, plasticized PLA

**Fig. 1** Visual appearance of: **a** PLA, **b** PLA-PEG, **c** PLA-ATBC, **d** PHB, **e** PLA-PHB, **f** PLA-PHB-PEG and **g** PLA-PHB-ATBC

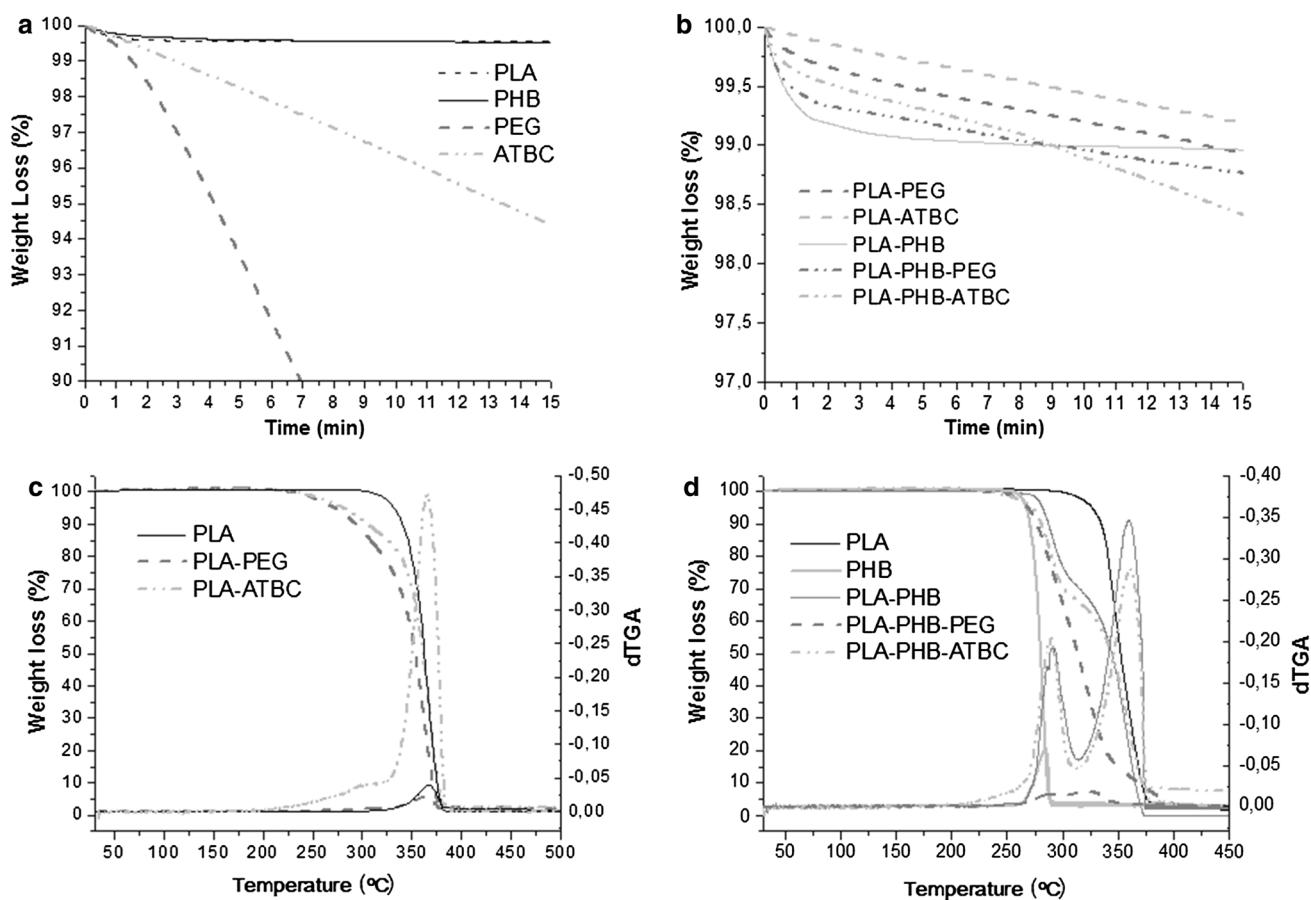
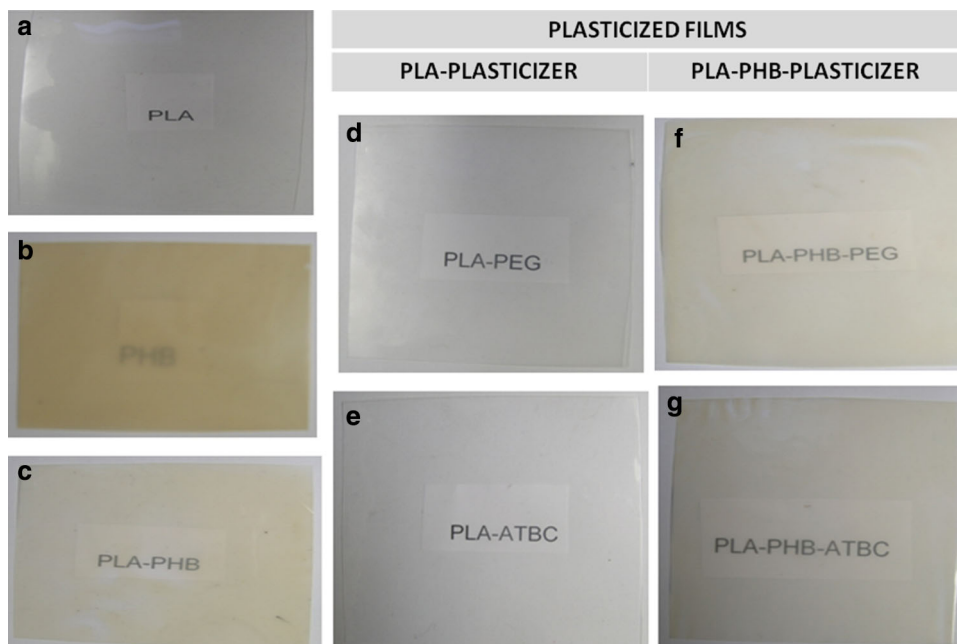


**Fig. 2** **a** TG isothermal curves of raw materials at 180 °C, **b** TG isothermal curves of blends at 180 °C, **c** TG and DTG dynamic curves of plasticized PLA and **d** TG and DTG dynamic curves of plasticized PLA-PHB

**Table 2** TG and DSC results

Formulation	TG and DTG parameters			DSC parameters			
	Stage	$T_0$ (°C)	$T_{max}$ (°C)	$T_g$ (°C)	$T_{cc}$ (°C)	$T_m$ (°C)	$\chi_c$ (%)
PLA	–	315	366	60.4	103.0	167.3	5.1
PLA–PEG	–	239	366	26.8	70.0	160.0	18.4
PLA–ATBC	–	245	365	34.6	74.1	161.3	8.1
PHB	–	261	285	–	–	174.2	40.7 <sup>a</sup>
PLA–PHB	I	272	291	58.1	105.2	167.4	16.4
	II	315	360				
PLA–PHB–PEG	I	250	285	25.1	64.2	160.2	36.5
	II	300	324				
PLA–PHB–ATBC	I	247	290	31.8	76.4	160.4	27.0
	II	313	361				

$T_0$ , calculated at 1 % mass loss (10 °C min<sup>-1</sup>)

<sup>a</sup>  $\chi_c$  (%), calculated using  $\Delta H_m^c$  of PHB

films degraded in a single step, while plasticized PLA–PHB blends degradation was a two-step process. In both cases a peak corresponding to the plasticizer vaporization was observed prior to the main degradation peak(s), as indicated for other plasticized polymers [42]. The first degradation process of the PLA–PHB blend was assigned to the PHB decomposition with onset temperature ( $T_0$ ) 272 °C and maximum degradation rate ( $T_{max}$ ) 291 °C (Table 2). PLA decomposition took place in the second stage at higher temperatures (onset 315 °C, maximum 360 °C). In this work, the values of  $T_0$  for the second degradation stage in PLA–PHB blends were estimated since this process was overlapped with the end of the first stage, characteristic of the PHB degradation. The addition of PHB resulted in the decrease of the PLA  $T_0$  value (Table 2). It was also observed that plasticized PLA–PHB showed higher  $T_0$  value than plasticized PLA films suggesting some stabilization of the PLA continuous phase caused by blending with PHB. It should be noted that the lowest value obtained for  $T_0$  was 239 °C for the PLA–PEG blend, temperature which is higher than those used in food processing or distribution, ensuring their thermal stability with no apparent degradation after processing.

PLA–PHB blends showed some increase in the  $T_{max}$  value corresponding to the PHB degradation, while  $T_{max}$  for the second stage was slightly lower than the value obtained for the neat PLA. It could be concluded that blending of PLA with PHB resulted in small modifications in their individual thermal stability, but not significant changes at processing and use temperatures were observed, ensuring the good thermal stability of these bio-films. In the case of the plasticized PLA–PHB blends, the addition of ATBC had no significant influence ( $p < 0.05$ ) on the thermal stability of the final formulation while the PLA–PHB–PEG film showed some decrease in the  $T_{max}$  value in the second degradation stage.

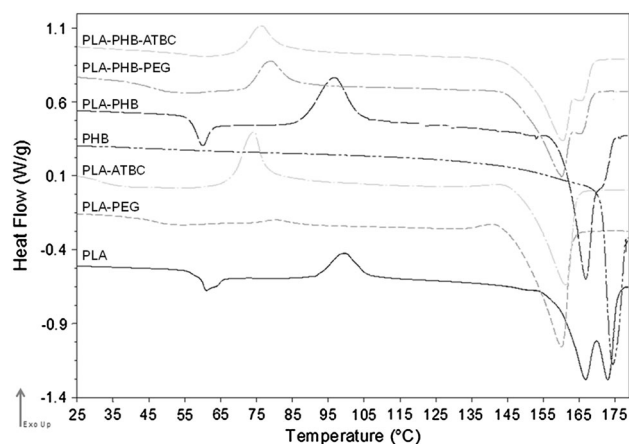


**Fig. 3** DSC thermograms during the first heating scan at 10 °C min<sup>-1</sup> for all formulations

#### Differential Scanning Calorimetry (DSC)

Figures 3 and 4 show the DSC thermograms for all samples, while Table 2 reports the numerical values of the main thermal events. Only one  $T_g$  value was observed for all formulations, suggesting the good miscibility between the different components in the amorphous region. A relevant shift to lower values in the  $T_g$  was observed for the PLA–PHB blend, giving another indication of the good interaction between both polymers after processing. A clear effect of the addition of ATBC or PEG to the polymer matrices was observed, since they induced the  $T_g$  depression in all plasticized films. This effect was due to their ability to increase the free volume between the polymer chains [23] and consequently their mobility. This reduction in  $T_g$  was higher in films plasticized with PEG, as expected, since plasticizers with low molecular weight are usually more efficient in lowering  $T_g$  values [28].

The endothermic peak corresponding to the enthalpic relaxation right after  $T_g$  was observed during the PLA and

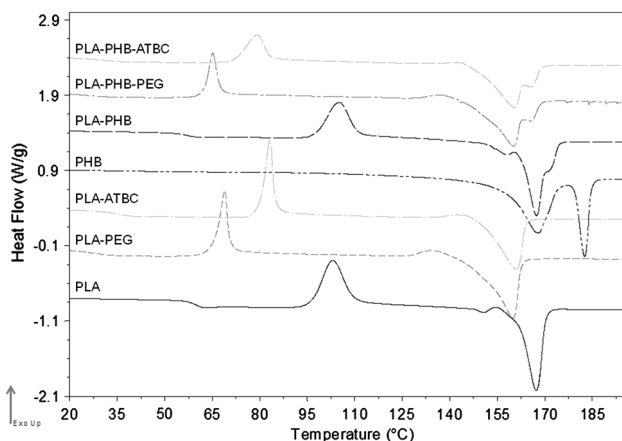


**Fig. 4** DSC thermograms during the second heating scan at  $10\text{ }^{\circ}\text{C min}^{-1}$  for all formulations

PLA–PHB first heating (Fig. 3). This peak can be related to the physical aging of polymers, probably PLA, before testing [43]. In these formulations the cold crystallization exotherm and two melting endothermic peaks were also observed. Double melting peaks in PLA films were related to the formation of crystalline structures with different perfection and thermodynamic stability [44, 45]. This behavior was previously observed in plasticized PLA formulations, since disordered  $\alpha'$ -crystals were formed when  $T_{cc}$  was around  $100\text{ }^{\circ}\text{C}$  [32, 46].

Recently Bartczak et al. [47] reported a decrease in a cold crystallization of PLA in with different proportions of PHB and ascribed this behavior to a partial miscibility between both polymers [47]. In this work, it was observed that  $T_{cc}$  shifted from  $103$  to  $105\text{ }^{\circ}\text{C}$  during the second heating scan, suggesting that PHB could promote the cold crystallization of the PLA matrix. As expected in plasticized materials, the incorporation of ATBC or PEG induced a higher decrease in  $T_{cc}$  due to the important increase in the polymers chain mobility. One of the goals of blending PLA with PHB is to increase the blends crystallinity to further control their properties. The crystallinity degree for all materials was calculated from DSC tests and results are reported in Table 2. As expected, the PHB film showed the highest  $\chi_c$ , while PLA–PHB blends increased their crystallinity in comparison to neat PLA, since PHB acted as nucleating agent of the PLA matrix [7]. In plasticized samples, PLA–ATBC films showed lower  $\chi_c$  evidencing the formation of amorphous materials in agreement with the visual aspect of highly transparent films (Fig. 1). Meanwhile, PLA–PEG films showed high  $\chi_c$  values and this could be related to the fact that PEG can interact with PLA resulting in higher chain mobility. Moreover, the macroscopic observation of PLA–PEG films showed that they were brittle, due to some phase separation

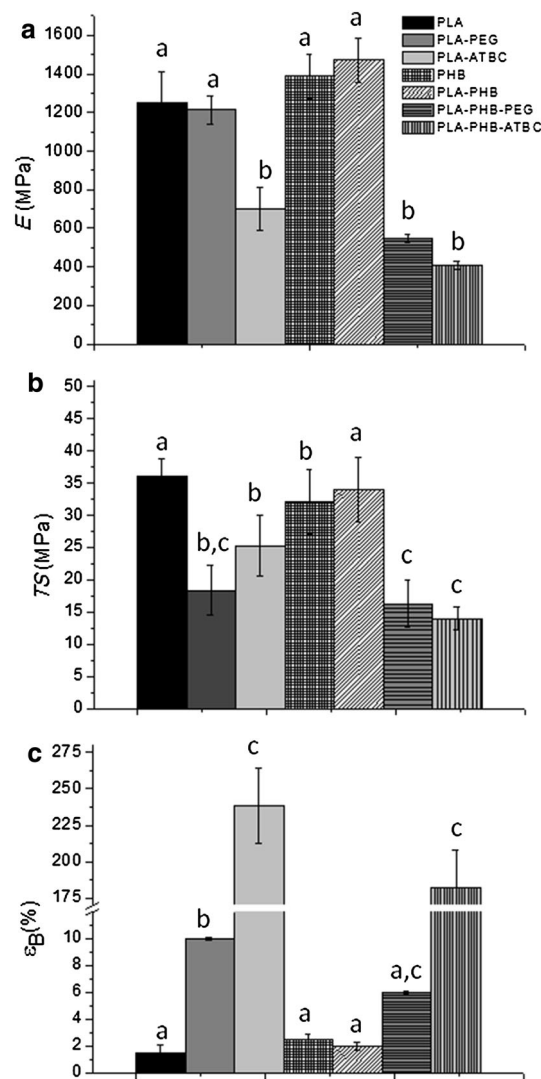


**Fig. 5** Modulus ( $E$ ), tensile strength ( $TS$ ) and elongation at break ( $\varepsilon_B$ ) of films ( $n = 5$ )

in these blends [23] induced by the increase in the crystalline phase [42]. This observation is in agreement with the higher differences observed between PEG and PLA solubility parameters.

#### Mechanical Properties

The influence of the addition of PHB and plasticizers in the tensile properties of PLA was evaluated. Results of the tensile properties for all formulations are shown in Fig. 5. Neat PLA and PHB showed similar elastic modulus ( $E$ ) values ( $p < 0.05$ ) while it slightly increased for the PLA–PHB blend due to the reinforcement effect of PHB, enhancing toughness (Fig. 5a). Moreover, the PLA–PHB blend showed comparable tensile strength ( $TS$ ) values to the PLA film ( $p = 0.05$ ) (Fig. 5b). As expected, all blends

with ATBC or PEG showed  $E$  and  $TS$  values lower than those for their unplasticized counterparts, since plasticizers induced ductile fracture, particularly in plasticized PLA–PHB films. These results are in good agreement with DSC tests where PLA–PHB–PEG and PLA–PHB–ATBC films showed lower  $T_g$  values than the plasticized PLA counterparts. These reductions of these mechanical properties for the PLA–PHB–ATBC formulation were significant ( $p > 0.05$ ), since these films showed a reduction in 70 % in  $E$  and 65 % in  $TS$  when compared with pure PLA.

A noticeable improvement in elongation at break ( $\epsilon_B$ ) was observed for plasticized PLA films (Fig. 5c), in full agreement with the decrease in their  $T_g$  values. This improvement was less pronounced for PLA–PHB films because of the reinforcement effect caused by the addition of PHB, while PLA, PHB and PLA–PHB films did not show stretchable behavior. It was also observed that ATBC produced much higher increase in  $\epsilon_B$  than PEG in all blends ( $p > 0.05$ ). In fact the addition of PEG did not show any clear improvement in ductile properties of PLA and/or PLA–PHB blends. A similar behavior was reported by Courgneau et al. [23] who observed that the addition of PEG resulted in the decrease in the PLA  $\epsilon_B$  due to the drop in PLA molar mass induced by PEG [23]. These results are in agreement with the clear increase in blends crystallinity already discussed by the addition of PEG to PLA-based formulations.

The higher plasticization effectiveness of ATBC for PLA and PLA–PHB matrices was in agreement with their high similarity in solubility parameters. These interactions resulted in a two-order of magnitude increase in  $\epsilon_B$  for the plasticized blends (from 1.5 % for PLA to 238 % for the PLA–ATBC film and from 2.0 % for the PLA–PHB blend to 182 % for the PLA–PHB–ATBC formulation). It should be noted that these values for  $\epsilon_B$  are similar to those of commercial plasticized PVC stretching films. Therefore, it could be concluded that PLA–ATBC and PLA–PHB–ATBC blends could be considered a sustainable alternative to current non-natural and non-biodegradable materials for food packaging films in terms of flexibility and possibilities for processing at the industrial level.

### Scanning Electron Microscopy (SEM)

Scanning electron microscopy (SEM) images of films surfaces (not shown) showed smooth surfaces for PLA and PHB films with no relevant heterogeneities. The PLA–PHB blend also showed homogeneous surface, with no apparent phase separation, suggesting the good interaction between both polymers in agreement with DSC results. As well, no apparent differences in surface homogeneity were observed in plasticized films surfaces, suggesting the good dispersion of plasticizers in both, PLA and PLA–PHB matrices.

Scanning electron microscopy (SEM) micrographs of fractured surfaces after tensile tests are shown in Fig. 6. Neat rigid fracture surfaces were clearly noticed for PLA, PHB and PLA–PHB films (Fig. 6 a–c), while plasticized samples showed ductile fracture patterns where plastic deformations were present, particularly in films plasticized with ATBC (Fig. 6B d–g). It is known that the introduction of relatively low-size molecules, such as those in ATBC, reduces molecular interactions between atoms in polymer chains [48], making easier the solubilization of the plasticizer into the polymer matrix resulting in a ductile behavior [40].

### Oxygen Transmission Rate (OTR)

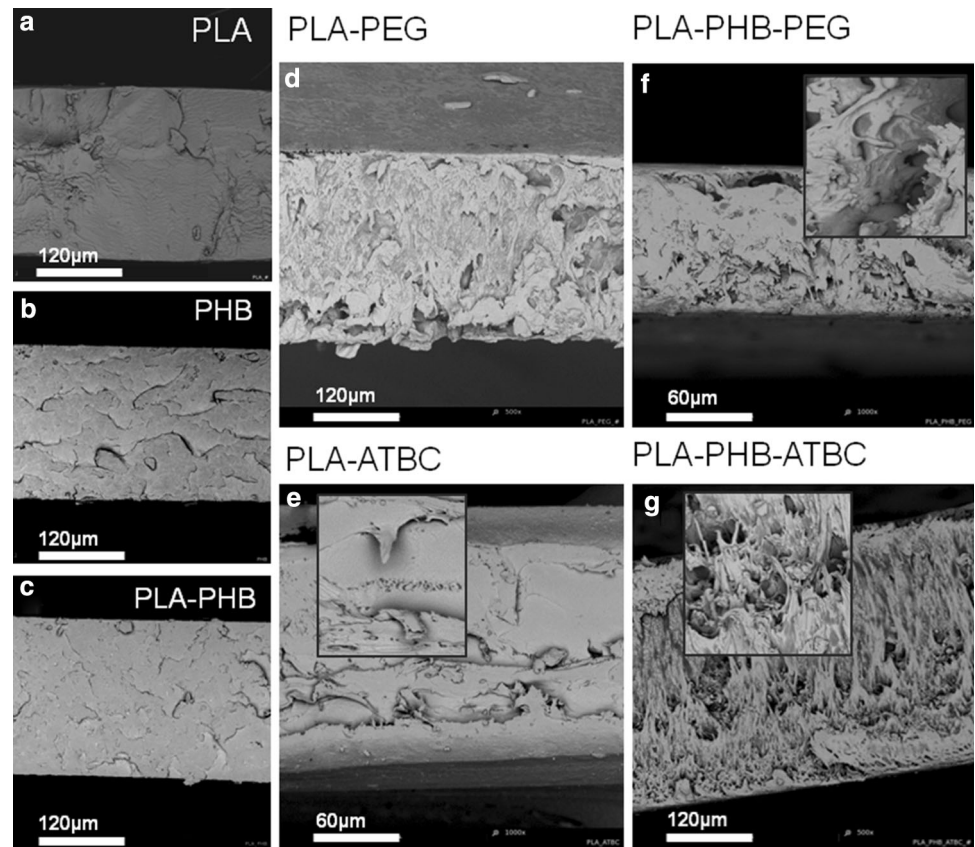
Oxygen barrier is one of the most important issues to be considered in materials intended to be used in food packaging, since the presence of oxygen in some cases and mainly for respiring foods (e.g. fruits and vegetables), it may lead to detrimental changes in quality and inducing a depression of food shelf-life [49]. OTR at the steady-state can be related to the oxygen permeation through the polymer structure and it is dependent on the film thickness. Thus, OTR· $e$  values were obtained and results are shown in Table 3. In general, PHB showed significant ( $p > 0.05$ ) higher barrier to oxygen than neat PLA, as expected from its higher intrinsic crystallinity and more efficient molecules distribution in the polymer structure. Therefore, the PLA–PHB blend resulted in improved barrier properties compared to neat PLA films. This effect could be caused by the increase in the PLA crystallinity by the addition of PHB.

It is well known that the addition of plasticizers to polymer matrices increases their oxygen transmission rate [4, 23, 32, 50]. In this case, films plasticized with PEG showed the highest OTR· $e$  values. Courgneau et al. already reported this effect and they concluded that PLA crystallization caused by physical aging might induce plasticizer segregation towards the amorphous phase and free volume around macromolecular chains in the polymer structure would increase [51].

The addition of PHB to the plasticized PLA matrix induced a general reduction in oxygen permeability, in particular for PLA–PHB–ATBC films, showing the good interaction between components in this ternary blend. However, no significant improvement in oxygen barrier was observed for the PLA–PHB–PEG film when compared to the PLA–PEG formulation ( $p < 0.05$ ). It should be noted that the OTR· $e$  results for these blends, particularly for those with PHB, suggested that these films could be used as sustainable materials for food packaging with values clearly lower than those calculated for low density polyethylene (LDPE),  $160 \text{ cm}^3 \text{ mm}^2 \text{ day}^{-1}$  [50] Even plasticized



**Fig. 6** Fractured SEM micrographs of: **a** PLA, **b** PHB, **c** PLA–PHB, **d** PLA–PEG, **e** PLA–ATBC, **f** PLA–PHB–PEG and **g** PLA–PHB–ATBC



formulations showed OTR results lower than those obtained for LDPE and plasticized PVC films (around  $80 \text{ cm}^3 \text{ mm m}^2 \text{ day}^{-1}$ ).

#### Total Soluble Matter

The weight difference between the initial dry matter and the material remaining after treatment in aqueous environments was determined by calculating the total soluble matter (TSM). Results are summarized in Table 3. PLA, PHB and PLA–PHB blends remained almost unaltered after treatment. Plasticized films showed a significant increase in water solubility that could be related to the plasticizer loss, which was clearly higher for PEG than for ATBC. It was also observed that the PLA–PHB blend was more effective preventing the plasticizer loss in aqueous environments than PLA due to the stabilization of the PLA continuous phase by blending with PHB, as it was previously discussed.

#### Water Contact Angle

Water contact angle measurements were used to evaluate the hydrophilic/hydrophobic behavior of these materials. Results are shown in Table 3. It is known that the water

contact angle increases with the surface hydrophobic character [40]. Thus, a water contact angle higher than  $65^\circ$  is typical in hydrophobic surfaces, while  $\theta^\circ$  values lower than  $65^\circ$  are obtained in hydrophilic materials [52]. Neat PLA and PHB showed hydrophilic surfaces, while PLA–PHB blends showed a significant improvement in their hydrophobic character with reduced water adsorption ( $p > 0.05$ ). In plasticized samples, the incorporation of PEG resulted in a slight decrease in the PLA contact angle suggesting some increase in the hydrophilic character, as it has been previously reported [53]. On the other hand, the contact angle for the PLA–ATBC film was around  $12^\circ$  higher, suggesting that the addition of ATBC produced some significant increase in the hydrophobic character of the PLA matrix ( $p > 0.05$ ). Similar results were observed in PLA and PLA–PHB incorporated with D-limonene, and this behavior was attributed to the hydrophobic character of this additive [4, 8]. The significant difference in the effect of plasticizers in PLA and PLA–PHB contact angles could be caused by their differences in water solubility. PEG is soluble in water while this is not the case for ATBC. Films plasticized with ATBC could be used in packaging formulations with reduced water absorption requirements since they showed higher hydrophobic character.

**Table 3** Yellow Index (YI), CIELAB color parameters, transparency, OTR-*e*, TSM and water contact angle measurements ( $\theta^\circ$ ) for all film formulations

Formulation	<i>L</i>	<i>a</i> *	<i>b</i> *	YI	$\Delta E^*$	<i>A</i> <sub>600</sub> /mm	OTR- <i>e</i> (cm <sup>3</sup> mm m <sup>-2</sup> day <sup>-1</sup> )	TSM	$\theta^\circ$
PLA	94.1 ± 0.1 <sup>a</sup>	-1.1 ± 0.1 <sup>ad</sup>	1.3 ± 0.1 <sup>a</sup>	3.5 ± 0.1 <sup>a</sup>	-	279.9 ± 2.8 <sup>a</sup>	44.1 ± 0.5 <sup>a</sup>	0.08 ± 0.01 <sup>a</sup>	58.4 ± 3.7 <sup>ac</sup>
PLA-PEG	91.1 ± 0.1 <sup>b</sup>	-0.8 ± 0.2 <sup>a</sup>	1.6 ± 0.1 <sup>a</sup>	4.2 ± 0.2 <sup>a</sup>	3.1 ± 0.2 <sup>A</sup>	264.5 ± 0.6 <sup>b</sup>	61.2 ± 1.4 <sup>b</sup>	8.57 ± 0.14 <sup>b</sup>	53.2 ± 3.4 <sup>a</sup>
PLA-ATBC	93.5 ± 0.1 <sup>a</sup>	-0.8 ± 0.1 <sup>a</sup>	1.4 ± 0.1 <sup>a</sup>	3.8 ± 0.1 <sup>a</sup>	0.7 ± 0.1 <sup>A</sup>	263.7 ± 0.1 <sup>b</sup>	51.8 ± 1.2 <sup>c</sup>	0.92 ± 0.02 <sup>c</sup>	70.7 ± 1.3 <sup>b</sup>
PHB	83.3 ± 2.2 <sup>c</sup>	1.0 ± 1.0 <sup>b</sup>	22.5 ± 3.3 <sup>b</sup>	45.1 ± 3.1 <sup>b</sup>	-	237.7 ± 0.8 <sup>c</sup>	24.9 ± 1.3 <sup>d</sup>	0.09 ± 0.04 <sup>a</sup>	61.3 ± 2.5 <sup>c</sup>
PLA-PHB	89.1 ± 1.0 <sup>d</sup>	-1.3 ± 0.1 <sup>ac</sup>	10.9 ± 2.1 <sup>c</sup>	21.7 ± 3.1 <sup>c</sup>	10.8 ± 2.0 <sup>A</sup>	259.3 ± 0.1 <sup>d</sup>	11.0 ± 0.7 <sup>e</sup>	0.08 ± 0.06 <sup>a</sup>	70.0 ± 0.6 <sup>d</sup>
PLA-PHB-PEG	89.5 ± 0.5 <sup>bd</sup>	-1.6 ± 0.2 <sup>cd</sup>	9.4 ± 0.7 <sup>c</sup>	18.5 ± 1.2 <sup>c</sup>	1.7 ± 0.5 <sup>B</sup>	240.4 ± 0.1 <sup>c</sup>	62.9 ± 1.3 <sup>b</sup>	7.41 ± 0.08 <sup>d</sup>	57.2 ± 2.0 <sup>ac</sup>
PLA-PHB-ATBC	89.8 ± 0.5 <sup>bd</sup>	-1.2 ± 0.3 <sup>ad</sup>	9.5 ± 0.8 <sup>c</sup>	19.1 ± 1.4 <sup>c</sup>	1.6 ± 0.5 <sup>B</sup>	236.8 ± 0.7 <sup>c</sup>	22.8 ± 2.8 <sup>d</sup>	0.50 ± 0.05 <sup>e</sup>	66.9 ± 3.1 <sup>b</sup>

<sup>a-c</sup> Different superscripts within the same column indicate significant differences between formulations (*p* < 0.05)

<sup>A</sup> Calculated by using PLA film color coordinates as control reference

<sup>B</sup> Calculated by using PLA-PHB film color coordinates as control reference

### Transparency and Colorimetric Properties

It was noticed that the addition of PHB to the transparent and colorless PLA films resulted in changes in color getting some yellowish tone (Fig. 1). The determination of transparency and color parameters in the CIELab space would permit to quantify these changes. Results are shown in Table 3. Neat PLA showed the highest transparency and *L* value, characteristic of the high brightness of PLA films. The addition of plasticizers significantly affected transparency (*p* < 0.05) of polymer films, but no significant differences between PEG and ATBC were observed, either in PLA or PLA-PHB blends. Furthermore, the plasticizer addition resulted in *a*\* values close to zero, while YI and *b*\* slightly increased and some decrease in *L* was also observed (*p* < 0.05).

PHB films showed the lowest transparency and *L* values and the highest *b*\* and YI values. In consequence, PLA-PHB blends showed some color differences with neat PLA, but some improvement in transparency and lightness when compared to neat PHB. No significant differences in *L* between the PLA-PHB blends and their plasticized counterparts were observed. In addition, PLA-PHB films showed some increase in the yellow color, with intermediate *b*\* values between neat PLA and neat PHB. In general, the addition of plasticizers contributed to improve the colored aspect of blends, decreasing their yellowness index and slightly increasing their transparency, which is an important consumer's requirement in food packaging applications.

### Conclusions

PLA was melt blended with PHB to increase crystallinity and further plasticized with PEG and ATBC to evaluate the possibility to obtain bio-based and biodegradable flexible films with improved properties for food packaging. Transparent and homogeneous films were obtained by melt-blending followed by compression molding processes. The addition of PHB increased the PLA crystallinity and the obtained PLA-PHB blends showed improved oxygen barrier properties and lowered water incorporation. Moreover, PHB improved the interface interaction between PLA and plasticizers. Those blends plasticized with ATBC showed higher flexibility and thermal stability than those with PEG. The best properties for the intended use in films manufacturing were found for the PLA-PHB-ATBC formulation, with moderate elongation at break, slightly amber color but still mostly transparent, reduced surface water absorption and a considerable improvement in oxygen barrier. In order to assess the use of these formulations in films manufacturing for biodegradable food packaging,

migration studies in different environments as well as disintegrability under composting conditions are currently on-going.

**Acknowledgments** This work has been supported by the Spanish Ministry of Economy and Competitiveness (MAT2011-28648-C02-01 and MAT2011-28468-C02-02) M.P. Arrieta is Granted by Santiago Grisolia program (GRISOLIA/2011/007). Authors gratefully acknowledge Prof. Arturo Horta Zubiaga from National University of Distance Education (UNED) Spain for his valuable discussion.

## References

- Erceg M, Kovacic T, Klaric I (2005) *Polym Degrad Stabil* 90:313–318
- Briassoulis D, Dejean C (2010) *J Polym Environ* 18:384–400
- Averous L (2004) *J Macromol Sci C* 44:231–274
- Arrieta MP, López J, Ferrandiz S, Peltzer M (2013) *Polym Test* 32:760–768
- Auras R, Harte B, Selke S (2004) *Macromol Biosci* 4:864
- Fortunati E, Armentano I, Zhou Q, Iannoni A, Saino E, Visai L, Berglund LA, Kenny JM (2012) *Carbohydr Polym* 87:1596–1605
- Zhang M, Thomas NL (2011) *Adv Polym Tech* 30:67–79
- Arrieta MP, López J, Hernández A, Rayón E (2014) *Eur Polym J* 33:289–296
- Arrieta MP, Parres-García FJ, López-Martínez J, Navarro-Vidal R, Ferrándiz S (2012) *DYNA* 87:395–399
- Almenar E, Samsudin H, Auras R, Harte J (2010) *J Sci Food Agr* 90:1121–1128
- Conn RE, Kolstad JJ, Borzelleca JF, Dixler DS, Filer LJ, Ladu BN, Pariza MW (1995) *Food Chem Toxicol* 33:273–283
- Fortunati E, Armentano I, Iannoni A, Kenny JM (2010) *Polym Degrad Stabil* 95:2200–2206
- Martino VP, Jimenez A, Ruseckaite RA, Averous L (2011) *Polym Advan Technol* 22:2206–2213
- Jamshidian M, Tehrany EA, Imran M, Jacquot M, Desobry S (2010) *Compr Rev Food Sci F* 9:552–571
- Hwang SW, Shim JK, selke SEM, Soto-Valdez H, Matuana L, Rubino M, Auras R (2012) *Polym Int* 61:418–425
- Calvao PS, Chenal J-M, Gauthier C, Demarquette NR, Bogner A, Cavaille JY (2012) *Polym Int* 61:434–441
- Malinova L, Brozek J (2011) *J Therm Anal Calorim* 103:653–660
- Ni C, Luo R, Xu K, Chen G-Q (2009) *J Appl Polym Sci* 111:1720–1727
- Vogel C, Siesler HW (2008) *Macromol Symp* 265:183–194
- Chang L, Woo EM (2012) *Polym Eng Sci* 52:1413–1419
- Tavera-Quiroz MJ, Urriza M, Pinotti A, Bertola N (2012) *J Sci Food Agr* 92:1346–1353
- Parra D, Rodrigues J, Ponce P, Lugao A (2005) *Pakistan J Biol Sci* 8:1041–1044
- Courgneau C, Domenek S, Guinault A, Averous L, Ducruet V (2011) *J Polym Environ* 19:362–371
- Baiardo M, Frisoni G, Scandola M, Rimelen M, Lips D, Ruffieux K, Wintermantel E (2003) *J Appl Polym Sci* 90:1731–1738
- European Food Safety Authority (2013) *EFSA Journal* 11:3245
- European Food Safety Authority (2012) *EFSA Journal* 10:2563
- Labrecque LV, Kumar RA, Dave V, Gross RA, McCarthy SP (1997) *J Appl Polym Sci* 66:1507–1513
- Liu H, Zhang J (2011) *J Polym Sci Pol Phys* 49:1051–1083
- Coltelli M-B, Della Maggiore I, Bertold M, Signori F, Bronco S, Ciardelli F (2008) *J Appl Polym Sci* 110:1250–1262
- Kulinski Z, Piorkowska E (2005) *Polymer* 46:10290–10300
- Martin O, Averous L (2001) *Polymer* 42:6209–6219
- Burgos N, Martino VP, Jiménez A (2013) *Polym Degrad Stabil* 98:651–658
- Martino VP, Ruseckaite RA, Jimenez A (2009) *Polym Int* 58:437–444
- Auras RA, Singh SP, Singh JJ (2005) *Packag Technol Sci* 18:207–216
- Corre Y-M, Bruzaud S, Audic J-L, Grohens Y (2012) *Polym Test* 31:226–235
- ASTM, “Standard Test Method for Tensile Properties of Thin Plastic Sheeting.”, ASTM Book Stand. 08.01:316., Philadelphia, PA., 1993 p. ASTM D882-91-01
- Martucci JF, Ruseckaite RA (2010) *J Food Eng* 99:377–383
- Molinaro S, Romero MC, Boaro M, Sensidoni A, Lagazio C, Morris M, Kerry J (2013) *J Food Eng* 117:113–123
- Auras R, Harte B, Selke S (2006) *J Sci Food Agr* 86:648–656
- Wu L-Y, Wen Q-B, Yang X-Q, Xu M-S, Yin S-W (2011) *J Sci Food Agr* 91:1222–1229
- Murariu M, Ferreira ADS, Alexandre M, Dubois P (2008) *Polym Advan Technol* 19:636–646
- Martino VP, Ruseckaite RA, Jiménez A (2006) *J Therm Anal Calorim* 86:707–712
- Gamez-Perez J, Velazquez-Infante JC, Franco-Urquiza E, Pages P, Carrasco F, Santana OO, MasPOCH ML (2011) *Express Polym Lett* 5:82–91
- Fortunati E, Armentano I, Iannoni A, Barbale M, Zaccheo S, Scavone M, Visai L, Kenny JM (2012) *J Appl Polym Sci* 124:87–98
- Scaffaro R, Botta L, Passaglia E, Oberhauser W, Frediani M, Di Landro L (2013) *Polym Eng Sci*. doi:10.1002/pen.23724
- Zhang J, Tashiro K, Tsuji H, Domb AJ (2008) *Macromolecules* 41:1352–1357
- Bartczak Z, Galeski A, Kowalczyk M, Sobota M, Malinowski R (2013) *Eur Polym J* 49:3630–3641
- López J, Parres F, Rico I, Molina J, Bonastre J, Cases F (2010) *J Therm Anal Calorim* 102:695–701
- Cagnon T, A Méry, P Chalier, C Guillaume, N Gontard (2014) *Innov Food Sci Emerg*
- Martino VP, Jimenez A, Ruseckaite RA (2009) *J Appl Polym Sci* 112:2010–2018
- Courgneau C, Domenek S, Lebosse R, Guinault A, Averous L, Ducruet V (2012) *Polym Int* 61:180–189
- Arrieta MP, Peltzer MA, López J, Garrigós MdC, Valente AJM, Jiménez A (2014) *J Food Eng* 121:94–101
- Tu Q, Wang J-C, Liu R, Zhang Y, Xu J, Liu J, Yuan M-S, Liu W (2013) *J Wang Colloid Surface B* 102:331–340